1984

A comparison of three Magnetic Anomaly Detection (MAD) models.

Schluckebier, Daniel Carl

Monterey, California. Naval Postgraduate School

NAVAL POSTGRADUATE SCHOOL
Monterey, California

THESIS

A COMPARISON OF THREE MAGNETIC ANOMALY DETECTION (MAD) MODELS

By

Daniel Carl Schluckebier

March 1984

Thesis Advisor: R. N. Forrest

SECURITY CLASSIFICATION OF THIS PAGE (When Date Entered)

REPORT DOCUMENTATION PAGE

READ INSTRUCTIONS BEFORE COMPLETING FORM

1. REPORT NUMBER	2. GOVT ACCESSION NO. / 3. RECIPIENT'S CATALOG NUMBER
4. TITLE (and Subtitle): A Comparison of Three Magnetic Anomaly Detection (MAD) Models	5. TYPE OF REPORT & PERIOD COVERED: Master's Thesis, March 1984
	6. PERFORMING ORG. REPORT NUMBER
7. AUTHOR(s): Daniel Carl Schluckebier	8. CONTRACT OR GRANT NUMBER(s)
9. PERFORMING ORGANIZATION NAME AND ADDRESS: Naval Postgraduate School, Monterey, California 93943	10. PROGRAM ELEMENT, PROJECT, TASK AREA & WORK UNIT NUMBERS
11. CONTROLLING OFFICE NAME AND ADDRESS: Naval Postgraduate School, Monterey, California 93943	12. REPORT DATE: March 1984
	13. NUMBER OF PAGES: 61
14. MONITORING AGENCY NAME & ADDRESS (if different from Controlling Office)	15. SECURITY CLASS. (of this report)
	15a. DECLASSIFICATION/DOWNGRADING SCHEDULE

16. DISTRIBUTION STATEMENT (of this Report)

Approved for public release, distribution unlimited

17. DISTRIBUTION STATEMENT (of the abstract entered in Block 20, if different from Report)

18. SUPPLEMENTARY NOTES

19. KEY WORDS (Continue on reverse side if necessary and identify by block number)

Magnetic Anomaly Detection, MAD, Cross-Correlation Detection Model, Square Law Detection Model, Definite Range Law Detection Model, Lateral Range Curves, Submarine Magnetic Signal, Submarine Magnetic Moments

20. ABSTRACT (Continue on reverse side if necessary and identify by block number)

This thesis presents a comparison of three Magnetic Anomaly Detection (MAD) models: a cross-correlation detection model, a square law detection model, and a model referred to as the OPTEVFOR detection model. FORTRAN and BASIC programs for the three detection models are included in this thesis. The programs yield detection probabilities for straight line encounters. Magnetic signal values for the straight line encounters are an additional output. Plots of lateral range curves and magnetic signal

DD FORM 1 JAN 73 1473 EDITION OF 1 NOV 65 IS OBSOLETE

S/N 0102-LF-014-6601

SECURITY CLASSIFICATION OF THIS PAGE (When Date Entered)

Block 20 (Cont)

values are presented. A discussion of the required parameters is included in the thesis to facilitate the use of the programs. The parameters that were considered in the comparison of the three detection models are: magnetic noise, aircraft and submarine headings, submarine displacement, and the vertical separation between submarine and aircraft.

Approved for public release, distribution unlimited

A Comparison of Three Magnetic Anomaly Detection (MAD) Models

by

Daniel Carl Schluckebier
Lieutenant, United States Navy
B.S., University of Nebraska, 1973

Submitted in partial fulfillment of the
requirements for the degree of

MASTER OF SCIENCE IN OPERATIONS RESEARCH

from the

NAVAL POSTGRADUATE SCHOOL
March 1984

ABSTRACT

This thesis presents a comparison of three Magnetic Anomaly Detection (MAD) models: a cross-correlation detection model, a square law detection model, and a model referred to as the OPTEVFOR detection model. FORTRAN and BASIC programs for the three detection models are included in this thesis. The programs yield detection probabilities for straight line encounters. Magnetic signal values for the straight line encounters are an additional output. Plots of lateral range curves and magnetic signal values are presented. A discussion of the required parameters is included in the thesis to facilitate the use of the programs. The parameters that were considered in the comparison of the three detection models are: magnetic noise, aircraft and submarine headings, submarine displacement, and the vertical separation between submarine and aircraft.

TABLE OF CONTENTS

LIST OF TABLES

LIST OF FIGURES

I. INTRODUCTION

This thesis presents a comparison of three Magnetic Anomaly Detection (MAD) models. The comparison is in terms of probabilities of detection that were computed using the models. Two of the models, the cross-correlation model and the square law model, have been used to model sonar detection [Ref. 1: pp. 343-357]. The third model, referred to as the OPTEVFOR model, is a slant range threshold detection model. The results of the comparisons are presented in graphical and tabular form. In addition, plots of magnetic signals for selected lateral ranges and noise levels are shown. The effects of noise, aircraft and submarine headings, submarine displacement, and vertical separation are also indicated.

The models were implemented using the FORTRAN and BASIC programs[1] that are listed in Appendix A. For those interested in using the programs for other investigations, an input parameter discussion is provided in Chapter 3. To use the FORTRAN program, the user specifies the input parameters in an input file. After execution of the program, an output file is generated that contains

---

[1]The programs are based on an unpublished BASIC program by R.N. Forrest for an H.P.- 85 microcomputer.

probabilities of detection for each of the three models. In addition, magnetic signal values and magnetic signal values plus random magnetic noise values for one of the encounters generated by the program are included in the output file. An IBM GRAFSTAT graphical package was used to produce the graphics in this thesis.

To use the BASIC program, the user must interactively enter the input parameter values for each encounter. After execution of the program, an optional hardcopy printout supplies the input parameter values and a table of detection probabilities for each of the three models (see Appendix A). Following this, lateral range curves are displayed to the user for immediate observation. A typical program run producing 21 detection probabilities for each model requires approximately 10 minutes of computing time on an Atari 800 microcomputer.

II. MODEL DESCRIPTIONS

A. THE CROSS-CORRELATION AND SQUARE LAW DETECTION MODELS

The cross-correlation and square law detection models are described in detail by Forrest [Ref. 2: pp. 33-35]. The models are based on the following assumptions: the noise is gaussian, and the signal sample points are such that adjacent magnetic noise samples are independent.

The magnetic signal values, as measured by an aircraft's magnetometer for the cross-correlation and square law detection models, are the submarine magnetic field values in the direction of the earth's magnetic field at the positions of the magnetometer. The submarine's field is assumed to be a dipole field, and the aircraft and the submarine are assumed to keep constant speeds and headings during an encounter.

For the cross-correlation model, a complete prior knowledge of the magnetic signal is required. Operationally, this suggests that a signal file, which contains a replica of the signal for each possible encounter situation, would be required. The model describes a perfect detection system with respect to the noise model that is used. For the square law model, a signal replica is not required. This model might be considered to describe

the limiting detection capability for an automatic system that does not use information about the shape of the magnetic signal.

B. OPTEVFOR MAD DETECTION MODEL

The OPTEVFOR model is described by Forrest [Ref. 3: pp. 7-8]. In characterizing the submarine magnetic signal as a simple dipole signal, the U.S. National Defense Research Committee, [Ref. 4: p. 20], reports that the magnetic signal of the submarine "varies as the inverse cube of the distance from the source". In an OPTEVFOR report [Ref. 5: p. 1, encl. 1], the results of a regression analysis on empirical peak to peak signal output against slant range between submarines and aircraft are reported. These results also suggested this inverse cube relationship for the magnetic signal. This relationship is the basis for the OPTEVFOR detection model.

The model has a deterministic mode and a stochastic mode, each of which involves the following parameters: the submarine magnetic moment (M), an Operator Recognition Factor (ORF), the average peak to peak magnetic noise (N) in the operating area, and a slant range (R). The relationship between these quantities is given by:

$$R = \left[\frac{c\,M}{(ORF)\,N} \right]^{1/3} . \qquad \text{(eqn 2.1)}$$

The value of the constant c is 0.10 for M in oersted centimeters^3, R in meters, and N in gamma.

In the deterministic mode, detection occurs if and only if the aircraft's slant range from the submarine at CPA is less than or equal to R. This mode yields a rectangular ("cookie cutter") lateral range curve with the probability of detection equal to 1 for an encounter where the slant range at CPA is less than or equal to R, and 0 when it is greater than R.

The stochastic mode allows a more uncertain approach to detection by allowing a gradual rise in probability of detection as the slant range at CPA decreases. In this mode one sets the probability of detection at R equal to 50 percent, and the lateral range curve is given by $p_d = \Phi(x)$; where it is understood that Φ is the standard normal cumulative distribution function and x is determined by the following equation:

$$x = \frac{R - CPA}{(AL)\,R} \quad . \qquad \text{(eqn 2.2)}$$

In this equation, CPA is the magnitude of the slant range distance at CPA, and R is the calculated range from Equation 2.1. The product (AL)R represents a standard deviation. The value of AL can be considered to be determined by "the combined uncertainty and variability in the values of M, N, and ORF" [Ref. 3: p. 8]. Two values of AL (.20 and .01) are shown in Figure 2.1. If empirical data was available, the

value of AL could be chosen to provide a best fit to the observed results. Note, as AL approaches 0, the stochastic mode approximates the deterministic mode.

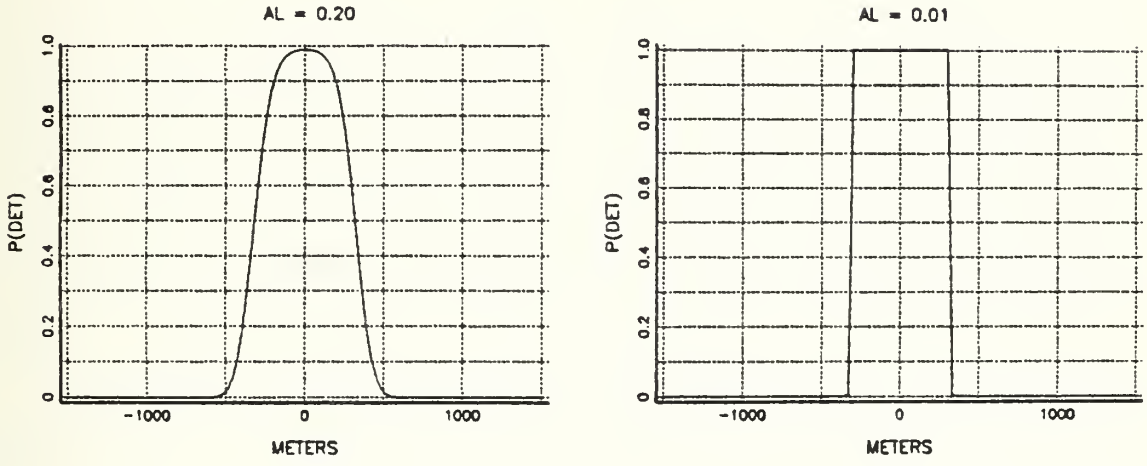

Figure 2.1. Lateral Range Curves for Different Values of AL.

III. INPUT PARAMETERS

The input parameters for the FORTRAN program are all contained in one input file. This allows parameter values to be easily changed without recompiling the main program or subroutines. Also, with a few changes, this program could be altered to operate in conjunction with a larger program to yield a probability of detection on an individual MAD run.

The input parameters are divided into four areas for discussion. They are: (1) sample interval, (2) earth magnetic field, (3) submarine moments, and (4) other inputs.

A. SAMPLE INTERVAL

The choice of a sample interval is discussed by Forrest [Ref. 2: pp. 27-30]. In the program, the total observation time in seconds over which the samples are taken is entered in T7. This time should be long enough to encompass a "complete signal" at the maximum expected detection slant range.

As the slant range from the submarine to the magnetometer increases, the distance over which a significant magnetic signal is present at the magnetometer also increases. Figure 3.1 graphically shows the difference

in the amount of time that a signal is present for slant ranges of 200 meters and 805 meters. In this thesis, the total time for a straight line encounter is assumed to be 20 seconds. As can be be seen from Figure 3.1, a 20 second interval adequately covers the significant portion of the magnetic signal for an 805 mmeter slant range at CPA.

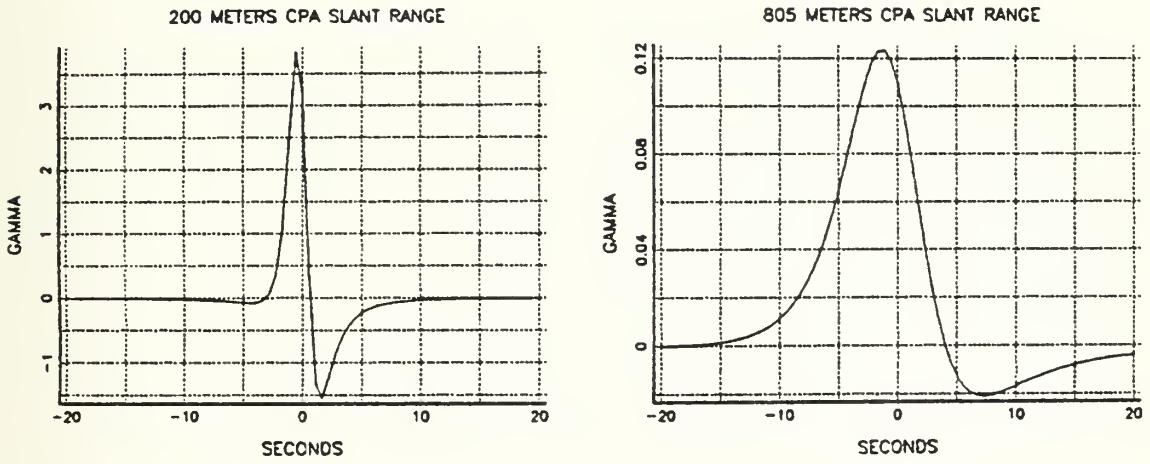

Figure 3.1. Magnetic Signals for Slant Ranges of 200 Meters and 805 Meters.

The time between samples is set equal to the reciprocal of twice the upper bandpass filter frequency of the MAD sensor. A value of 0.9 Hz was suggested for use by Texas Instruments [Ref. 6: p. 112] as an upper bandpass filter limit in a discussion on the effects of noise on a MAD system. This value yields a time interval between samples of 0.55 seconds.

The sample interval length and the false alarm rate (the expected number of false alarms per hour) determine the

false alarm probability. The false alarm rate (F2) is assigned a value of 3 based on a report by OPTEVFOR [Ref. 5: p. 2.1].

B. EARTH MAGNETIC FIELD

Input values for the earth magnetic field intensity and inclination, or dip angle, may be taken from two Defense Mapping Agency Hydrographic Center charts, [Refs. 7 and 8 respectively], or approximated by using a program. If chart values are entered, the earth field intensity must be in units of gamma and the inclination in decimal degrees. The program used to determine the intensity of the earth field and inclination is based on a simple dipole field model that is described by Forrest [Ref. 9: pp. 39-43].

Table III-1 displays the program output values of inclination in decimal degrees and earth magnetic field in gamma for selected geographic locations. In addition, corresponding values obtained from the Defense Mapping Agency Hydrographic Center Charts Number 30 and Number 39 are also displayed. The last three columns are the average slant range in meters at which a 50 percent probability of detection is obtained for the three program detection models. The program input parameters for these slant ranges were the same as the base case, except for the following differences: a sample interval time of 40 seconds, aircraft and submarine headings of 0 degrees, and a submarine

Table III-1

Slant Detection Ranges for the Three Detection Models to Compare the Inclination and Earth Magnetic Field Model Values to DMAHC Chart Values

Latitude	Longitude	Inclination in decimal degrees		Earth Magnetic Field in oersted*		Slant Detection Ranges in Meters		
		Program	Chart#30	Program	Chart #39	Cross-Correlation	Square Law	OPTEVFOR
60	180	74		.63		650	422	282
			70		.53	629	419	278
60	90	82		.68		615	346	264
			84		.61	566	308	246
30	150	58		.51		718	487	310
			50		.41	707	482	304
30	60	59		.53		711	482	308
			59		.48	688	469	298
30	-60	31		.39		799	542	326
			45		.46	772	524	324
30	-150	42		.43		770	524	322
			40		.40	762	518	318
0	30	9		.35		834	563	328
			-5		.28	767	514	306
0	-60	-25		.38		815	550	326
			-20		.37	827	559	328
-30	90	-30		.39		703	472	304
			-34		.31	718	487	298
-60	30	-69		.60		671	444	292
			-56		.34	621	424	274

*one oersted = 10^5gamma.

displacement of 7,000 tons. The correlation between the slant ranges, comparing the chart values and model values, was found to be 95 to 96 percent for the three models. This suggests that, even though differences exist between the chart values and model values, there is a high degree of correlation in the final output.

A limitation to the simple dipole field model is that it does not give an angle of declination (variation) with sufficient accuracy.[2] As a result, all headings entered into this program must be in magnetic degrees. The Phoenix Corporation [Ref. 10: pp. 24-25] reports on geomagnetic field models that can represent the earth field "with overall accuracies better than approximately 150-200 gammas in magnitude and .2° in direction of the field." This degree of accuracy is not needed for this program, but a simplified version of one of these models that provided satisfactory angles of declination would be beneficial if the program were to be incorporated into a larger model that utilized true headings as inputs.

C. SUBMARINE MAGNETIC DIPOLE MOMENT

If a submarine's magnetic dipole moment is known for the geographical location and the submarine's magnetic heading,

---

[2]Private communication from R.N. Forrest, who investigated the use of the simple dipole model for this purpose.

the following values may be entered in the program: (1) P, its magnitude in oersted centimeters cubed, (2) A, its direction in decimal degrees relative to magnetic north, and (3) B, its depression angle from the horizontal in decimal degrees. If it is not known, these values must be calculated for a specific location and magnetic heading. A program is included in the main program that can be used to calculate these values. The program is based on a model described by Forrest [Ref. 9: pp. 35-38]. The input to the program is submarine displacement in tons. The program also contains coefficients which relate displacement to magnetic moment. The values used in the program are based on values cited by Texas Instruments [Ref. 6: p. 4].

The past history of the submarine is represented by the permanent longitudinal, transverse, and vertical moments of the submarine (M4, M5 and M6 in oersted centimeters cubed). For the examples in this thesis, it was assumed that effective deperming had been performed and program default values of zero were used.

D. OTHER PARAMETERS

1. Headings and Speeds

Since the simple dipole earth field model used by the program does not produce accurate angles of declination, magnetic headings are required. In addition, the headings

must be in decimal degrees. The input parameters for submarine speed and aircraft speed are entered in knots.

2. Noise

The magnetic noise is assumed to be such that adjacent magnetic noise samples are independent. This assumption is based in part on the filtering that is performed on the magnetic signal by the processing system in a MAD detection sensor. The standard deviation of the noise in units of gamma is the value entered into S1. This value can be approximated from operational data by taking from one-fourth to one-sixth of the measured peak to peak magnetic noise. [Ref. 2: pp. 28-29]

The OPTEVFOR detection model incorporates a value of average peak to peak magnetic noise (N) in the inverse cube law calculation. In the program, the value of N is determined by multiplying the S1 entry by four.

3. Operator Recognition Factor (ORF)

The ORF is the value of the ratio of magnetic signal to magnetic noise for which the average operator would detect a signal 50% of the time in the presence of background noise for a false alarm rate of 3 per hour. An ORF value of 3 was suggested for use by OPTEVFOR [Ref. 5: p. 4.12].

4. Distance Parameters

Two parameters, R8 and N7, are used to define the points plotted on the lateral range curves. R8 is the

maximum positive value of the lateral range in meters for which a lateral range curve value is to be computed. N7 represents the number of lateral range curve values that are to be computed from the maximum lateral range to zero lateral range.

The vertical separation (Z) is the sum of the submarine depth and aircraft altitude in meters.

IV. RESULTS

Program outputs of the three models for a set of base case conditions are presented in this section. Outputs for variations from the base case are also presented. The lateral range of an encounter (the horizontal separation between the submarine and magnetometer when the magnetometer is at CPA) for a 50% probability of detection is used as a measure of comparison. Signal and signal plus "noise" traces for several cases are presented. The traces are based on the signal and noise models that are part of the cross-correlation and square law models. These idealized signal traces appear to have the characteristics of actual signal traces. This suggests that the signal and noise models might be used for training purposes.

A. BASE CASE

The base case conditions are listed in Table IV-1. The table is ordered in the same manner that the values are read into the program. An annotation of each entry is included for clarity.

Figure 4-1 presents the lateral range curves for the base case. Points on the lateral range curves are indicated by the first letter of the name of the model from which they were derived. The slight asymmetry of the cross-correlation

detection model and square law detection model curves is reflective of the shape of the signals that are 'received' in these models.

Table IV-1. Input Parameters for the Base Case

1.8	twice the upper bandpass limit in seconds
20.0	sampling time interval in seconds
3.0	false alarms per hour
0	Enter inclination (1 = yes, 0 = no)?
30.0	area of operation latitude in decimal degrees
60.0	area of operation longitude in decimal degrees
45.0	submarine magnetic heading in decimal degrees
10.0	submarine speed in knots
315.0	aircraft magnetic heading in decimal degrees
220.0	aircraft speed in knots
0	Enter submarine moment (1 = yes, 0 = no)?
0	Enter earth field (1 = yes, 0 = no)?
0	Enter submarine perm moments (1= yes, 0 = no)?
4000.0	submarine displacement
200.0	vertical separation in meters
0.1	noise (standard deviation) in gamma
1500.0	maximum lateral range in meters
50.0	divisions of lateral range
3.0	ORF (Operator Recognition Factor)
0.2	variability factor for OPTEVFOR model
0025	lateral range iteration number for the magnetic signal and signal plus noise in the output file

Table IV-2 lists lateral detection ranges and corresponding slant detection ranges at CPA for a probability of detection equal to 50 percent for the cross-correlation and square law detection models. An equivalent ORF value for each model is also listed. Due to the asymmetry of the lateral range curves for the cross-correlation and square law models, the average of the two 50

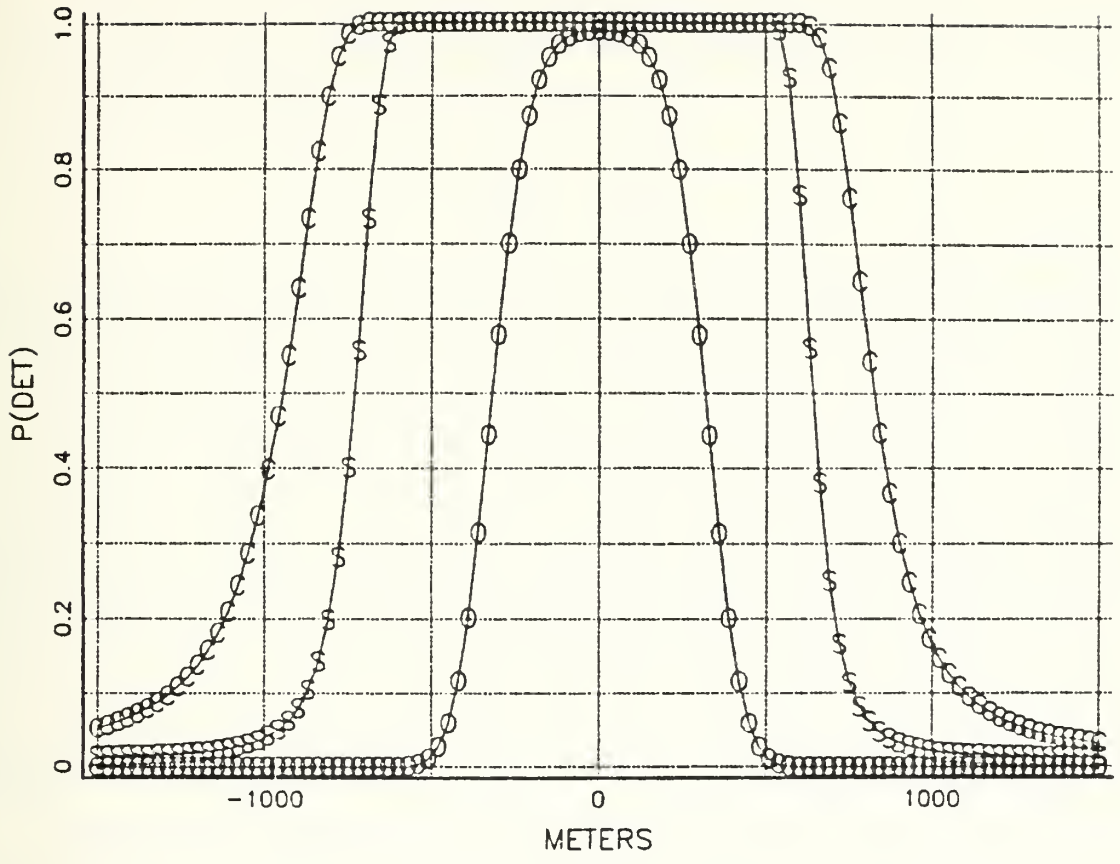

Figure 4-1. Lateral Range Curves of the Cross-Correlation (C), Square Law (S), and OPTEVFOR (O) Models for the Base Case.

Table IV-2. The Lateral Detection Ranges, Slant Detection Ranges, and ORF's of the Three Models for the Base Case.

	Lateral Detection Range (meters)	Slant Detection Range (meters)	ORF
Cross-Correlation	885	907	.21
Square Law	685	714	.44
OPTEVFOR	318	376	3

percent detection ranges was used as the lateral detection range. The equivalent ORF values for the cross-correlation

and square law detection models were calculated using the slant detection range values with the following equation, which was obtained from Equation 2.1:

$$ORF = \frac{c\ M}{R^3\ N} \quad . \qquad \text{eqn 4.1}$$

For the base case, the magnitude of the submarine field (M) at the submarine is 6.35×10^8 orested-cm^3, the noise (N) is .4 gamma, and the value of the constant (c) is .1. This suggests that, in order to detect a magnetic signal 50 percent of the time with a false alarm rate of 3 per hour, the magnetic signal to magnetic noise ratio should be .21 for an ideal cross-correlation detector and .44 for an ideal square law detector.

Using the ORF values, the cross-correlation and square law detection models can be used to describe the performance of an operator. To do this, a modified value of the standard deviation (σ) of the input noise can be used. The modified value is equal to (ORF)(σ)/.21 for the cross-correlation detection model and (ORF)(σ)/.44 for the square law detection model. With these modifications, the two models can be used to describe the detection capability of an operator with a specified ORF. An example of a lateral range curve with the modified noise standard deviation for an ORF of 3 is presented in Figure 4.2 for each model. These curves are comparable to the lateral range curve for the OPTEVFOR model that is shown in Figure 4.1.

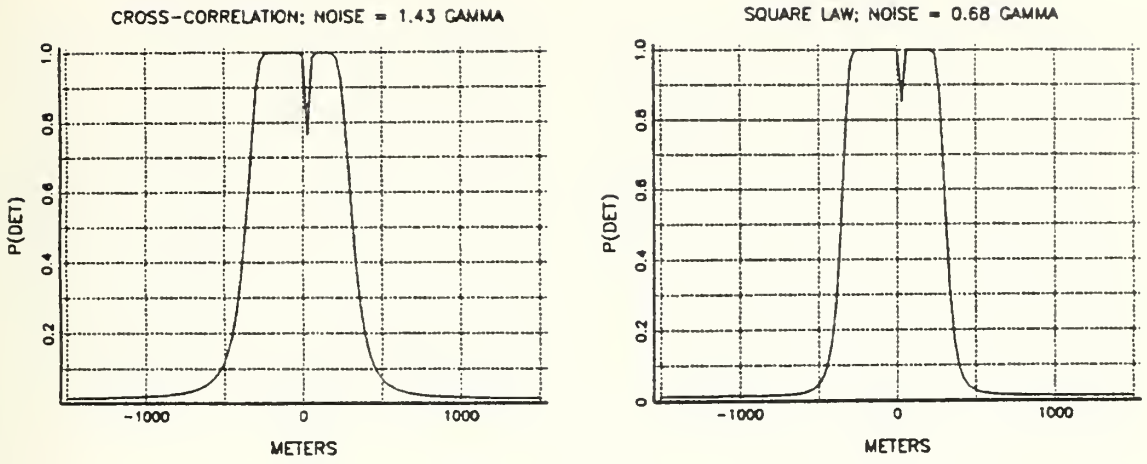

Figure 4.2. Cross-Correlation and Square Law Lateral Range Curves to Describe the Performance of an Operator with an ORF of 3.

The automatic MAD system manufactured by Canada's CAE Electronics Ltd. is expected to produce a 50 percent increase in detection slant range [Ref. 11]. Using the detection slant range for the OPTEVFOR model of 376 meters, a 50 percent improvement would yield a detection slant range of 564 meters. The ORF for a detection system with this capability would be .88. The cross-correlation and the square law detection models could be used to yield lateral range curves for a system with an ORF of .88 by using a noise standard deviation equal to .88 (σ)/.21 and .88 (σ)/.44 respectively. Figure 4.3 shows the lateral range curves of the two detection models with a 50 percent improvement in slant range detection. Note, with the modified noise standard deviations, the models are essentially equivalent for the cases considered.

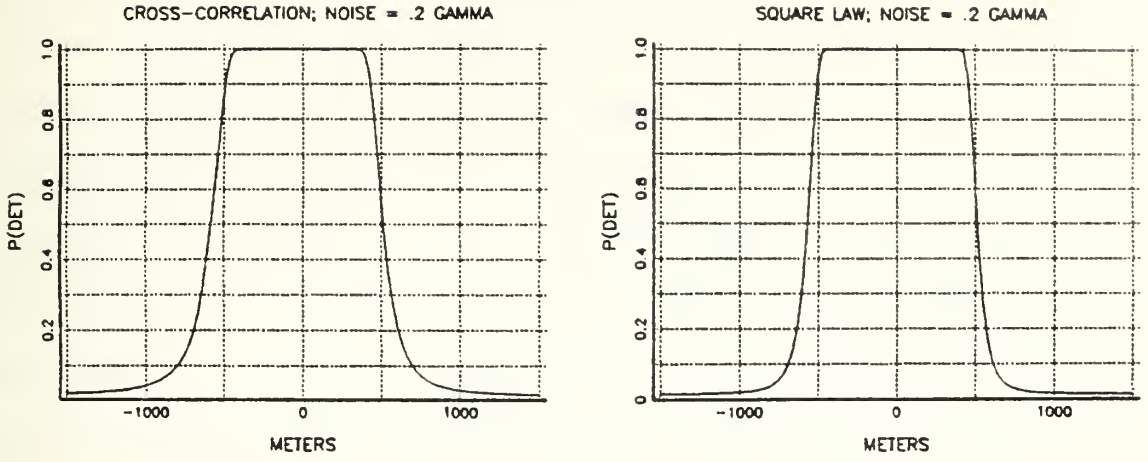

Figure 4.3. The Cross-Correlation and Square Law Models to Describe LRC's for the CAE Automatic Detection System.

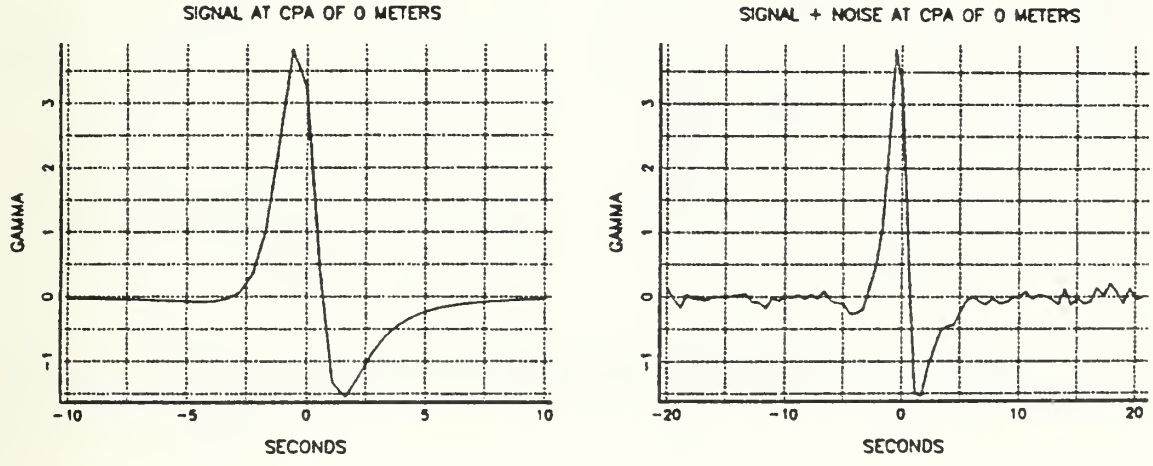

Figure 4.4. Magnetic Signal and Magnetic Signal Plus Magnetic Noise at a Lateral Range at CPA of 0 Meters for the Base Case.

Figures 4.4 and 4.5 present the magnetic signal and a representation of magnetic signal plus magnetic noise that would be received under the base conditions by a magnetometer with a lateral range of 0 meters and of 780

meters. The signal plus noise trace was generated from signal plus noise values obtained by adding a signal value to a gaussian noise value. The gaussian noise value was generated by multiplying the standard deviation of the input noise by a pseudo normal random number from a population with mean 0 and variance 1. The pseudo normal random numbers were generated using LLRANDOMII, a resident program at the Naval Postgraduate School computer [Ref. 12: p. 2.2].

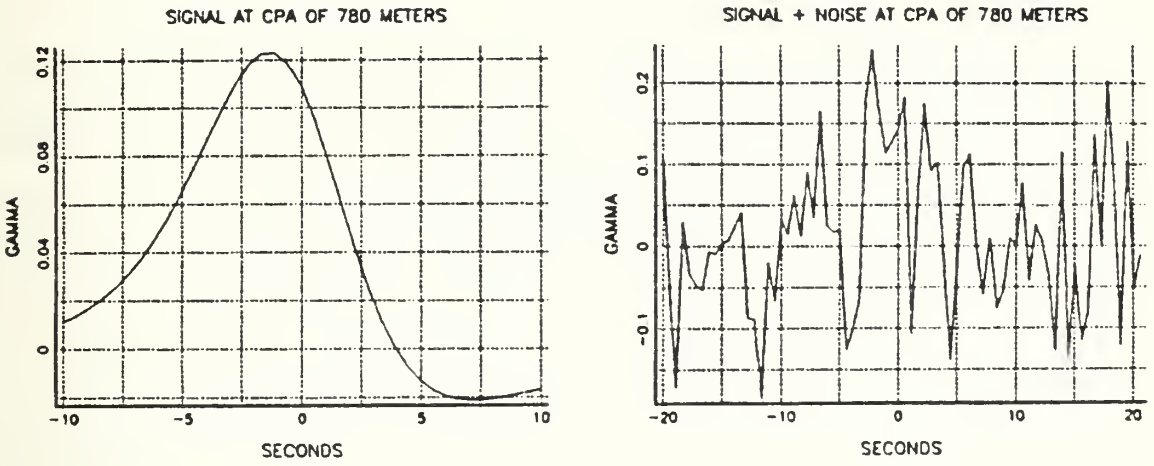

Figure 4.5. Magnetic Signal and Magnetic Signal Plus Magnetic Noise at a Lateral Range at CPA of 780 Meters for the Base Case.

The magnitude of the magnetic signal shown in Figure 4.4 is very large in comparison to the background noise. The peak to peak signal to noise ratio is approximately 14 to 1. An operator would have little difficulty identifying the signal in this signal plus noise trace.

Conversely, the magnetic signal shown in Figure 4.5 is small compared to the background noise. The peak to peak

signal to noise ratio is .35. The probabilities of detection for the lateral range of 780 meters are: .95 for the cross-correlation detection model, .28 for the square law detection model, and 0 for the OPTEVFOR detection model. It seems apparent that an operator would have a difficult, if not impossible, time in detecting this signal at a reasonable false alarm rate.

B. DIFFERENT NOISE INPUTS

The first variation on the base case shows the effect of different noise inputs. The standard deviation (σ) of the peak to peak noise is the input parameter that is varied. Table IV-3 lists the different σ values and the corresponding lateral detection ranges.

Table IV-3. The Effect of Noise on Detection Range.

Standard Deviation of Noise in Gamma	Lateral Detection Range in Meters		
	Cross-Correlation	Square Law	OPTEVFOR
.005	2250(2259)*	1792(1803)*	1000 (1020)*
.01	1832 (1843)	1446 (1460)	782 (807)
.05	1110 (1128)	868 (890)	427 (472)
.1	885 (907)	685 (714)	318 (375)
.5	512 (550)	382 (431)	90 (219)

*The numbers in parentheses are the slant range distances in meters. The vertical separation is 200 meters.

Figure 4.6 displays lateral range curves for the three models when the standard deviation of the noise is .01 gamma. These three curves show an increase in lateral

detection range over the base case. Note that the asymmetry of the cross-correlation and square law detection models is more apparent in Figure 4.6 than it was in Figure 4.1.

Figure 4.7 displays the magnetic signal (which is the same as the signal in Figure 4.5) and the magnetic signal plus magnetic noise at a horizontal distance of 780 meters when the magnetometer is at CPA. The signal to noise ratio is 3.5. The figure suggests that a MAD operator, in this case, should have the ability to detect a signal at 780 meters lateral range with a satisfactory false alarm rate.

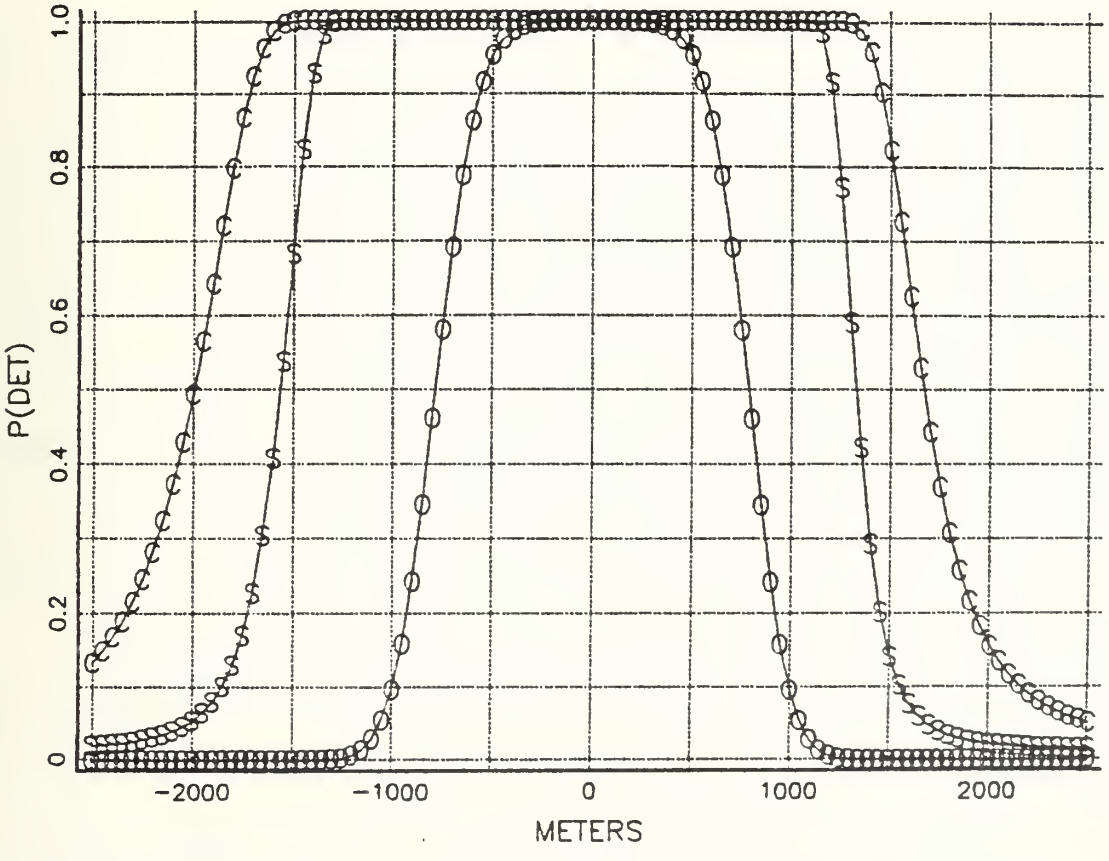

Figure 4.6. Lateral Range Curves for the Three Models with the Standard Deviation of the Noise Set to .01 Gamma.

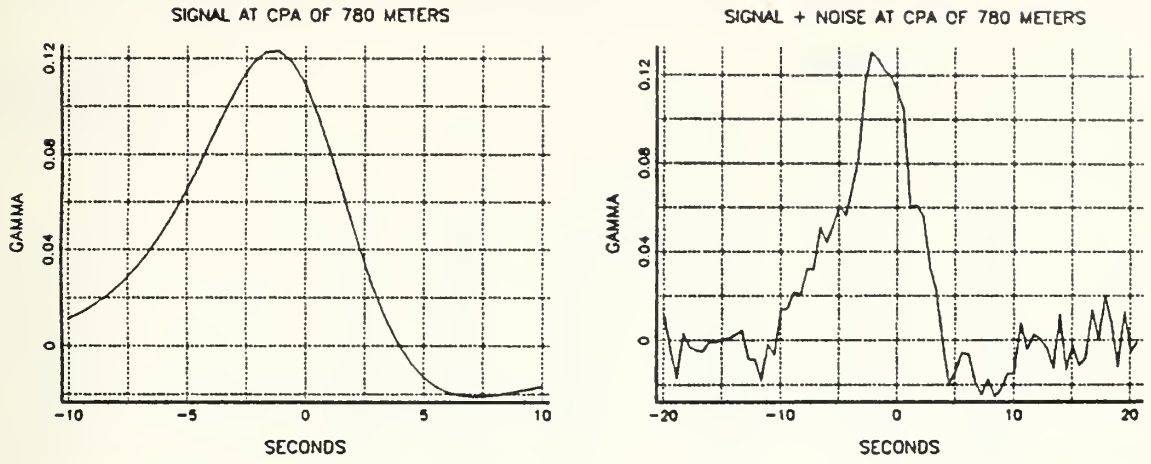

Figure 4.7. Magnetic Signal and Magnetic Signal Plus Magnetic Noise with the Standard Deviation of Noise = .01 Gamma at 780 Meters Lateral Range.

C. DIFFERENT HEADINGS

The headings of a submarine and an aircraft in an encounter have an effect on detection ranges. The effect of different headings was investigated using the square law detection model, and the results in terms of lateral detection ranges are presented in Table IV-4. This table suggests that a submarine should choose a magnetic heading of either East or West, and, for an encounter, an aircraft should also choose a magnetic heading of East or West.

Figure 4.8 shows lateral range curves for a submarine heading North and an aircraft heading East. In this case, both the cross-correlation and square law detection model lateral range curves display noticeable asymmetry. The OPTEVFOR detection model lateral range curve is symmetric

Table IV-4. Square Law Lateral Detection Ranges for Different Submarine and Aircraft Magnetic Headings

Aircraft Headings (magnetic)	Submarine Headings (magnetic)							
	0	45	90	135	180	225	270	315
0	700	650	498	640	686	640	498	650
45	724	637	505	670	713	624	501	676
90	730	654	527	654	730	646	524	646
135	712	685	505	636	724	682	502	624
180	685	640	498	650	700	650	498	640
225	712	624	501	672	724	636	506	672
270	730	646	519	646	730	654	533	654
315	724	685	501	624	713	682	505	636

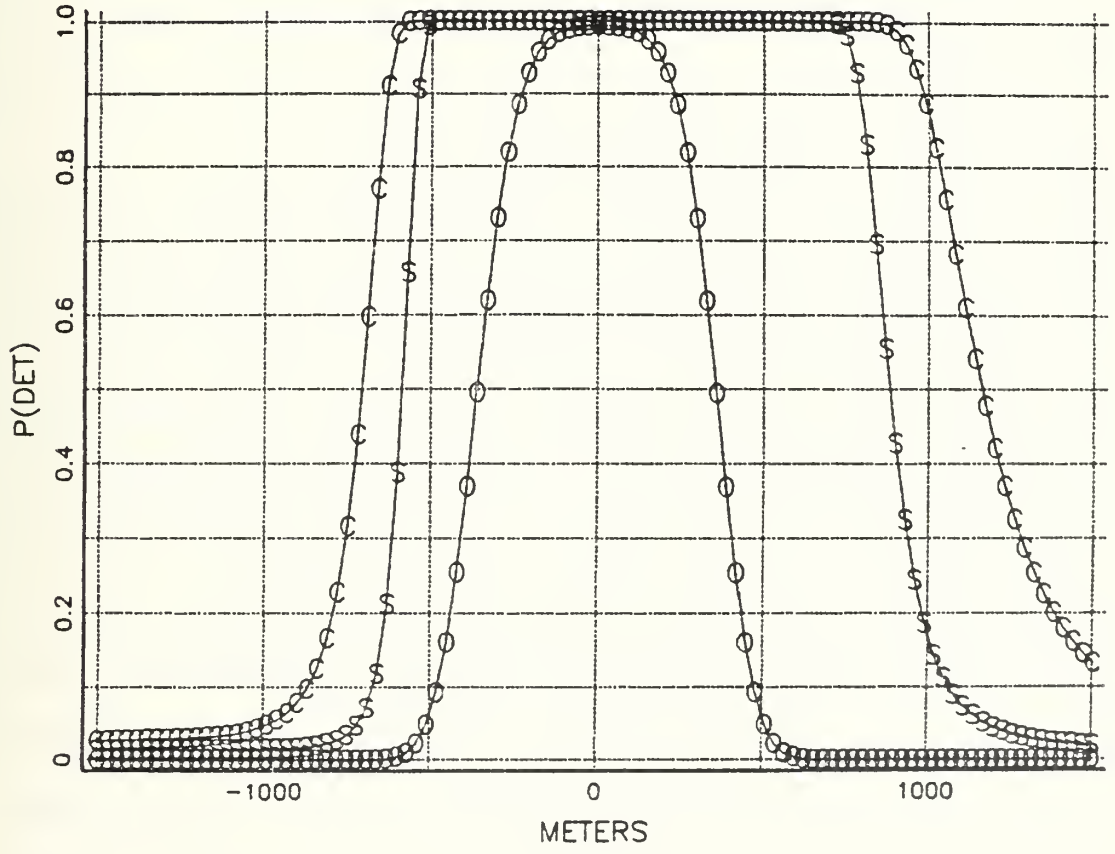

Figure 4.8. Lateral Range Curves for the Submarine Heading North and the Aircraft Heading East.

but, like the curves for the other models, it shows an increase in detection ranges over those for the base case (where the submarine is heading NE and the aircraft is heading NW).

The APAIR MOD 2.6 [Ref. 13: p. 83] simulation uses a MAD detection model that accounts for the change in a submarine's magnetic moment (which is dependent on changes in submarine heading) by using a parameter labeled DFACTR (degradation factor for heading). In the model, D (a modified slant range at CPA) determines the probability of detection. The value of D is determined using the following relation:

$$D = DC\ (1 - DFACTR \times A), \qquad \text{eqn. 4.1}$$

where DC is the slant range at CPA and A is the acute angle in decimal degrees between the submarine heading and an East-West bearing. The probability of MAD detection is determined from a table of probability of detection against slant range. A uniform (0, 1) random number is drawn to determine whether or not the submarine is detected. The average slant detection ranges (computed from Table IV-4, where the vertical separation is 200 meters) for submarine headings of North and East are 741 meters and 545 meters respectively. These ranges yield a value of .003 for DFACTR. The average slant detection range from Table IV-4 for a submarine heading of NE is 682 meters; however, the slant range determined by a modified slant range of 545

meters and a DFACTR = .003 is 643 meters. If sin A instead of A is used in Equation 4.1, then DFACTR is .265 and the slant detection for a submarine heading NE is 670 meters. Since this is only a single data point and there is no supporting operational data, the modification is not proposed as one that should be adopted. However, this cursory analysis does indicate a way in which the programs presented in this thesis might be used by others.

Table IV-5 lists lateral ranges for P(det) equal to 50 percent for 3 submarine/aircraft heading combinations. The cross-correlation and OPTEVFOR detection model results show the same relationship as the results of the square law detection model.

Table IV-5. Lateral Ranges for P(det) = .50 in Meters for the Three Detection Models.

Submarine	45	0	90
Aircraft	315	90	0
Cross-Correlation	885	934	754
Square Law	685	730	498
OPTEVFOR	318	358	230

For the detection ranges reported by OPTEVFOR [Ref. 5: p. 5.1], the effect of different headings was averaged out. That is, measurements were taken from the 16 possible combinations of the 4 cardinal submarine and aircraft headings in equal numbers and then averaged to yield an average slant detection range. But, as shown in Tables IV-4 and IV-5, the models show significant variability in lateral

detection range for different submarine and/or aircraft headings.

Figure 4.9 is included to show the lateral range curves when the submarine is headed East and the aircraft is headed North. These lateral range curves give the minimum lateral detection ranges for the different heading combinations. Also, for the cross-correlation and square law detection models, the lateral range curves are fairly symmetric.

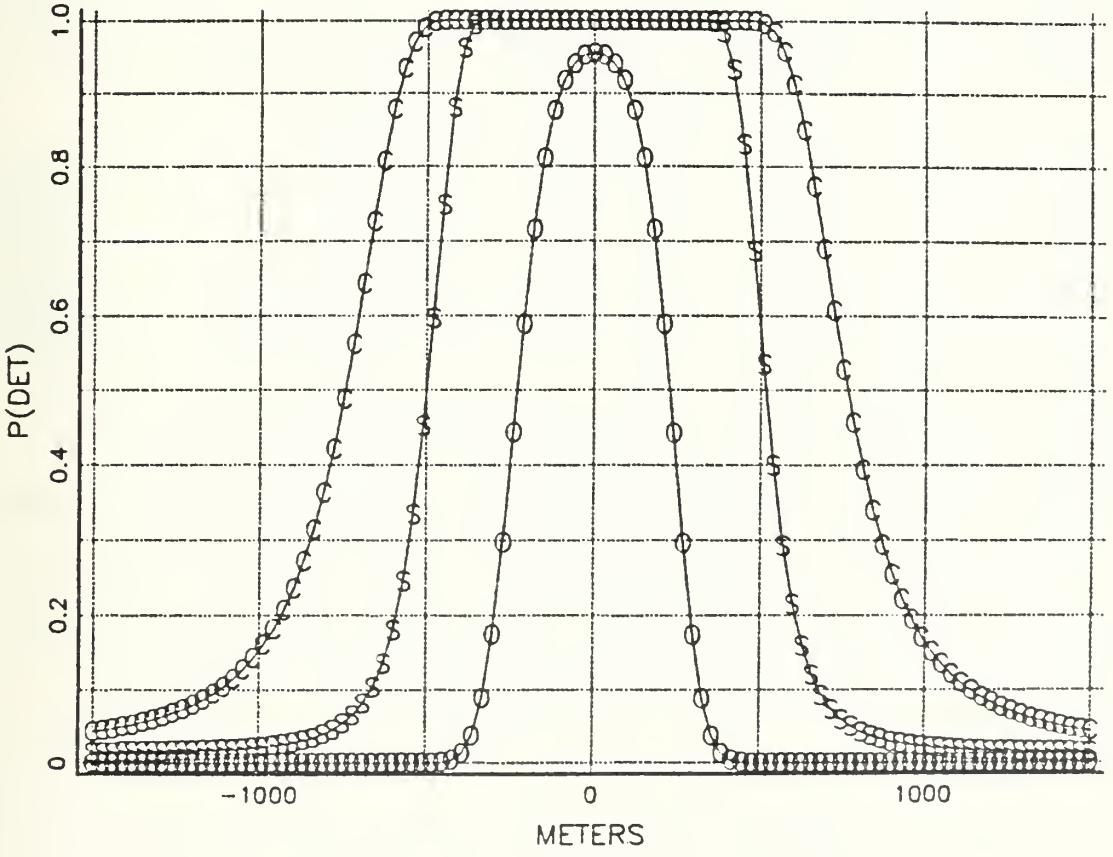

Figure 4.9. Lateral Range Curves for the Submarine Headed East and the Aircraft Headed North.

D. SUBMARINE DISPLACEMENT

The submarine magnetic dipole moment program within the main program is used to calculate a submarine's induced magnetic moments. The program is based on a model described by Forrest [Ref. 9: pp. 35-38]. The model requires submarine displacement as an input. Table IV-6 displays results when the submarine displacement is doubled in each succeeding entry.

Table IV-6. Slant Detection Ranges in Meters for Different Submarine Tonnages.

Displacement in tons	Signal Magnitude in oersted cm^3	Slant Detection Ranges in Meters Cross-Correlation	Square Law	OPTEVFOR
1000	1.59×10^8	590	463	236
2000	3.17×10^8	732	575	297
4000	6.35×10^8	907	714	376
8000	1.27×10^9	1127	885	472
16000	2.54×10^9	1402	1099	597
32000	5.08×10^9	1724	1363	753

As can be seen from column two in Table IV-6, the dipole moment is proportional to the displacement. Since the three detection models give a slant detection range that is proportional to the cube root of the dipole moment, doubling the submarine displacement should multiply the slant detection range by $2^{1/3}$ (1.26). This is confirmed by comparing the slant detection ranges between the entries in Table IV-6. Doubling the displacement multiplies the slant detection range by 1.24 for the cross-correlation and square

law detection models and, as expected, by 1.26 for the OPTEVFOR detection model.

Table IV-7 lists the displacement in tons of selected Soviet submarines. The values were taken from Combat Fleets of the World 1982/1983 [Ref. 14: pp. 602-614]. This table

Table IV-7. Selected Soviet Submarine Displacements.

Class	Displacement in Tons
Typhoon	25-30,000
Delta III	10,500-13,250
Yankee	8,000-9,600
Echo II	5,000-6,000
Victor I	4,300-5,100
Charlie I	4,000-4,900
Tango	3,000-3,700
Foxtrot	1,950-2,400
Whiskey	1,080-1,450

is presented solely for the purpose of the information it contains. The submarine magnetic dipole moment program should not be expected to give accurate estimates of these submarine's induced magnetic moments, since the program uses a value that relates displacement to magnetic moment that is based on submarines of World War II.

E. VERTICAL SEPARATION

Figure 4.10 shows three lateral range curves for a vertical separation of 500 meters. The OPTEVFOR detection model lateral range curve shows only a slight detection probability even when the aircraft passes directly over the submarine. The cross-correlation and square law detection model lateral range curves show an increase in lateral

detection range over the base case. The dip in the lateral range curves, for each of these models, suggests the complex variation of the magnetic signal with lateral range.

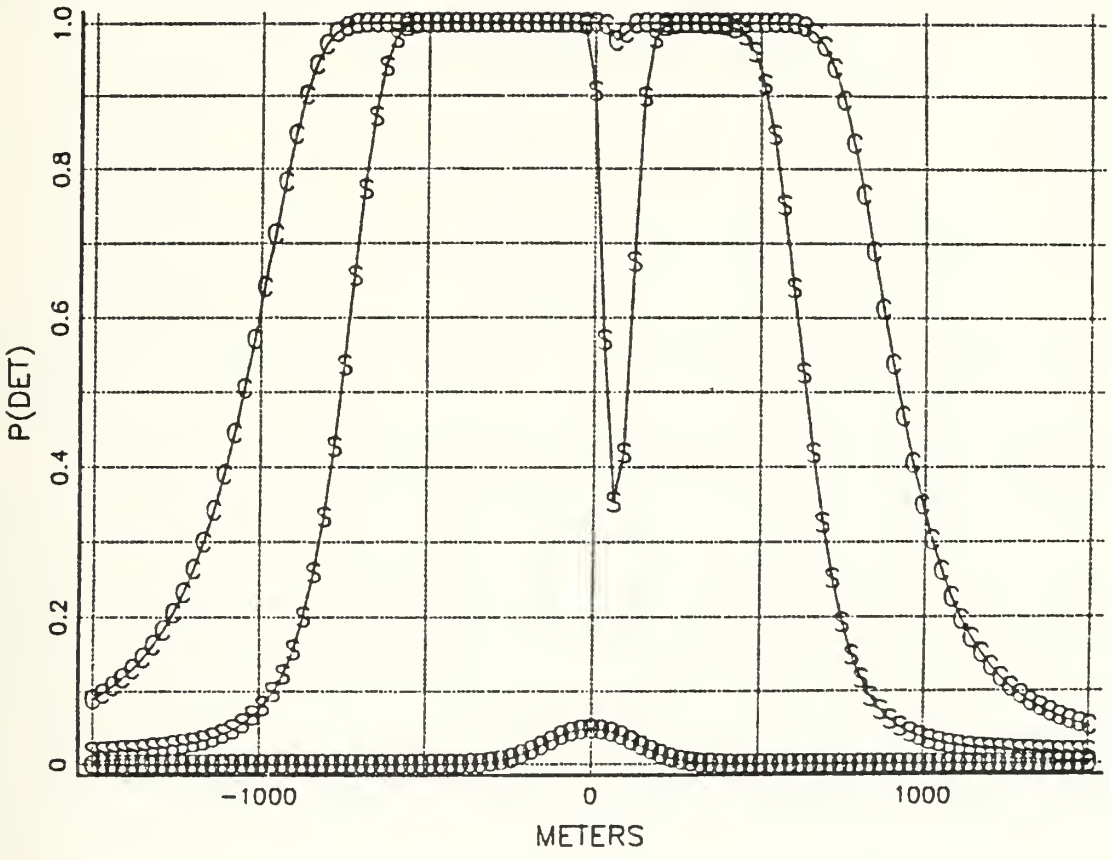

Figure 4.10. Lateral Range Curves for a Vertical Separation of 500 Meters.

Table IV-8 lists the lateral detection ranges for different vertical separations. It should be kept in mind that these values are for a single geographic location; consequently, they may not be representative of other locations. Note that both the cross-correlation and square

law detection models lateral detection ranges increase with an increase in vertical separation until about 500 meters.

Table IV-8. Lateral Detection Ranges for Different Vertical Separations.

Vertical Separation in meters	Lateral Detection Range in Meters		
	Cross-Correlation	Square Law	OPTEVFOR
100	804	614	360
200	885	685	318
300	942	720	225
400	974	724	--*
500	980	699	
600	974	629	
700	936	262	

*No longer attains a probability of detection equal to 50 percent.

A factor related to vertical separation is the effect of ocean wave noise on a MAD system. As the altitude of a magnetometer is decreased, the magnitude of the ocean wave noise increases. Because of the rate of this increase, for a given submarine and submarine depth there is a minimum altitude at which an aircraft should prosecute a submarine using MAD. Further investigation using an ocean wave noise model might be valuable.

V. CONCLUSIONS

This thesis has presented a comparison of three MAD detection models. The cross-correlation detection model, which models an optimum detector under the conditions of the detection model, yields the maximum detection range for a set of given conditions. The square law detection model does not describe an optimum detector under the conditions of the model and yields shorter detection ranges. In the stochastic mode, with an appropriate choice for the parameter AL that determines the standard deviation, the lateral range curves for the OPTEVFOR detection model become similar to the other two detection models. Detection ranges for the OPTEVFOR detection model depend on the choice for the Operator Recognition Factor (ORF). With a value of 3 for the ORF, it yields the shortest detection ranges. Adjusting the magnetic noise level by an amount proportional to the effective ORF, the cross-correlation and square law models can be used to describe the performance of an operator or an automatic detection system.

The magnetic signal and magnetic signal plus noise traces appear to have the characteristics of actual signal traces. This suggests that the signal and noise models, which are the basis for the cross-correlation and square law detection models, might be useful for training purposes.

Variations on a set of base case parameters were used to show relative changes in the detection models. The parameters included: magnetic noise, submarine and aircraft magnetic headings, submarine displacement, and vertical separation. Significant results were the large asymmetry of the lateral range curves under certain conditions and the variation of the magnetic signal as shown by the changes in vertical separation.

The FORTRAN and BASIC programs, along with an input parameter discussion, are included to facilitate the use of the three MAD detection models as they are implemented by the programs.

```
C   THIS IS A COMPUTER PROGRAM FOR THE COMPUTATION OF PROBABILITIES
C   OF DETECTION FOR THE CROSS-CORRELATION, SQUARE LAW, AND OPTIMUM
C   DETECTION MODELS.
C
      INTEGER H,M,AA,NN8,E,I,LL
C
      REAL  G(1000),D1(500),D2(500),K(500),X0(500),F1,T1,T7,G1,HH,F2,
     *L1,L2,L,O,F,H1,C90,J,K,R,Q,A,B,D3,P,V1,V2,C0,C1,C2,W1,W2,W0,DR,
     *E1,M4,M5,M6,K1,K2,K3,M9,M3,M8,M1,M2,M7,P1,X,Y,V6,V7,Z,S1,R8,
     *N7,N1,D4,N8,L9,PI,N,CRF,AL,D5(500),TN(500)
C
 10   FORMAT (F15.8)
 20   FORMAT('1','INPUT ERROR - LOWER MAX FREQ OR INT TIME.')
 30   FORMAT(I4)
 40   FORMAT('0','EARTH FIELD = ',F15.7)
 50   FORMAT(' MAG P=',F20.1,/,' HOR ANG=',F10.6,/,' VERT ANG=',F10.6)
 60   FORMAT(T1,'LTR RNG',T11,'PD(CC)',T19,'PD(SL)',T27,'PD(OP)',T39
     *,'G(I)',T48,'TN(I)')
 70   FORMAT(T1,F7.1,T11,F6.3,T19,F6.3,T27,F6.3,T37,F7.4,T47,F7.4)
 80   FORMAT('1','REL COURSE',F10.3,/,' REL SPEED',F10.3)
 90   FORMAT('1','PHI',F15.8)
100   FORMAT(T5,E15.8)
C
C   THIS PART OF THE PROGRAM INPUTS THE PARAMETERS FROM A MAD INPUT FILE.
C
      DR=57.29577951
      C90=90.0/DR
C   INPUT MAX FREQ AND INTERVAL TIME
C
      READ(4,10)F1
      T1=1.0/F1
      READ(4,10)T7
      G1=T7/2.0/T1
      H=IFIX(G1)
      HH=FLOAT(H)
      H=H+IFIX(2.0*(G1-HH))
      M=2*H+1
      IF(M.LT.500) GOTO 500
         WRITE(6,20)
         GOTO 580
 500  CONTINUE
      T7=T1*FLOAT(M)
C   INPUT FALSE ALARMS PER HOUR
      READ(4,10)F2
      HH=FLOAT(M)
      P1=F2*(HH-1.0)*T1/3600.0
C   INPUT MAG DIP ANGLE OR COMPUTE IT
      READ(4,30)AA
```

```
      IF(AA.EQ.0) GOTO 510
C  INPUT MAD MAG DIP ANGLE
      READ (4,10)F
      F=F/DR
      GOTO 515
  510 CONTINUE
C  COMPUTE AN APPROXIMATION OF DIP ANGLE
      L1=76.0/DR
      L2=100.0/DR
C  INPUT OP AREA LAT LONG
      READ (4,10)L
      READ (4,10)O
      L=L/DR
      O=O/DR
      F=SIN(O-L2)*COS(L)
      G1=COS(O-L2)*COS(L)
      H1=SIN(L)
      CALL ROTATE(G1,H1,J,K1)
      J=J-(C90-L1)
      G1=K1*SIN(J)
      H1=K1*COS(J)
      CALL ROTATE(G1,F,J,K1)
      F=K1
      R=-(COS(L1)*SIN(J))
      Q=-(COS(L1)*COS(J))
      CALL ROTATE(H1,F,J,K1)
      F=ATAN(2.0*TAN(J))
      WRITE(6,90)F
  515 CONTINUE
C  INPUT DIPOLE COURSE, C1 AND SPEED, V1.
      READ (4,10)C1
      C1=C1/DR
      READ (4,10)V1
C  INPUT SENSOR COURSE, C2 AND SPEED, V2.
      READ (4,10)C2
      C2=C2/DR
      READ (4,10)V2
      W1=V2*SIN(C2)-V1*SIN(C1)
      W2=V2*COS(C2)-V1*COS(C1)
      CALL ROTATE(W1,W2,C0,W0)
      WRITE(6,80)C0,W0
C  CO IS REL COURSE, WO IS REL SPEED
      D2=W0*T1*4.63/9.0
C  INPUT DIPOLE MOMENT OR APPROXIMATE BY COMPUTATION.
      READ (4,30)AA
      IF(AA.EQ.0) GOTO 520
C  INPUT MAGNITUDE P,HOR ANGLE,VERT ANGLE
      READ (4,10)F
```

```
      READ (4,10)A
      READ (4,10)E
      A=A/DR
      B=B/DR
         GOTO 560
  520 CONTINUE
C   INPUT EARTH FIELD OR APPROXIMATE
      READ (4,30)AA
      IF(AA.EQ.0) GOTO 530
         READ (4,10)E1
         GOTO 540
  530 CONTINUE
      E1=70000.0/SQRT(3.0*COS(F)*COS(F)+1.0)
  540 CONTINUE
      WRITE (6,40)E1
      M4=0.0
      M5=0.0
      M6=0.0
C   INPUT PERMANENT MOMENTS OR APPROXIMATE
      READ (4,30)AA
      IF(AA.EQ.0) GOTO 550
         READ (4,10)M4
         READ (4,10)M5
         READ (4,10)M6
  550 CONTINUE
      K1=7.3
      K2=1.6
      K3=1.6
C   INPUT DIPOLE DISPLACEMENT
      READ (4,10)N1
      M9=E1*K3*N1*SIN(F)
      M3=M9+M6
      M8=E1*COS(F)*N1*(K1*COS(C1)*COS(C1)+K2*SIN(C1)*SIN(C1))
      M1=M4*SIN(C1)+M5*COS(C1)
      M2=M4*COS(C1)-M5*SIN(C1)
      M7=E1*(COS(F)*(K1-K2)*N1*SIN(C1)*COS(C1))
      M1=M7+M1
      M2=M8+M2
      CALL ROTATE(M1,M2,A,V)
      CALL ROTATE(M3,V,B,P)
  560 CONTINUE
      WRITE (6,50)P,A,B
      CALL INORM1(P1,V6)
      V7=HH*(1.0-2.0/9.0/HH+V6*SQRT(2.0/9.0/HH))**3
C     WRITE(6,100)V6
C     WRITE(6,100)V7
C   INPUT VERT SEPARATION, NOISE, MAX LAT RANGE & NUMBER
C   OF INCREMENTS.
```

```
      READ(4,10)Z
      READ(4,10)S1
      READ(4,10)RE
      READ(4,10)N7
      N=4*S1
      READ(4,10)CRF
      READ(4,10)AL
      READ(4,30)LL
      D4=R8/N7
      N8=2.0*N7
      L9=-R8
      NN8=IFIX(NE)+1
      DO 570 E=1,NN8
         CALL SUM(L9,Z,B,CO,A,F,P,M,D3,SO,G,K1,N8,S1,LL,E,TN)
         XO(E)=L9
         CALL MCD3(P,N,CRF,AL,L9,D5,E,Z)
         L9=L9+D4
         CALL PRCE1(SO,K,VE,K1,S1,M,V7,D1,D2,E)
  570 CONTINUE
C   OUTPUT PROBS TO MAD OUTPUT FILE
      WRITE(7,60)
      DO 580 I=1,NN8
         WRITE(7,70)XO(I),D1(I),D2(I),D5(I),G(I),TN(I)
  580 CONTINUE
      STOP
      END
C
C   THIS SUBROUTINE COMPUTES THE MAGNITUDE OF THE SIGNAL FOR USE IN
C   THE TWO SIGNAL DETECTION THEORY MODELS.  IT ALSO RETURNS THE SIGNAL
C   OF A SELECTED (L) LATERAL RANGE IN THE GG VECTOR AND A TRACE OF A
C   SIGNAL PLUS RANDOM NOISE (WITH STANDARD DEV = SIGMA) IN THE
C   TN VECTOR.
C
      SUBROUTINE SUM(XO,Z,B,CO,A,F,P,M,D3,SO,GG,K1,N8,N,L,J,TN)
C
      INTEGER M,I,J,K,L
      REAL    XO,Z,D,HO,B,CO,A,F,P,D3,BO,JO,NO,B1,J1,N1,K1,A2,SO,
     *MM,II,S,Q,G,GG(100),TN(500),N8,N
C
      CALL ROTATE(XO,Z,C,HO)
      BO=COS(B)*COS(CO-A)
      JO=COS(D)*COS(B)*SIN(CO-A)-SIN(D)*SIN(B)
      NO=-(SIN(D)*COS(B)*SIN(CO-A))-COS(D)*SIN(B)
      B1=COS(F)*COS(CO)
      J1=COS(D)*COS(F)*SIN(CO)-SIN(D)*SIN(F)
      N1=-(SIN(D)*COS(F)*SIN(CO))-COS(D)*SIN(F)
      K1=P/12.0*HO**3
      A2=2.0 *BO*B1-JO*J1-NO*N1
```

```
      A1=3.0 *(NC*B1+B0*N1)
      AC=2.0 *N0*N1-B0*B1-J0*J1
      SC=0.0
      MM=FLOAT(M)-1.0
   20 FORMAT(T5,'TRACE OF ',I4)
      IF(J.NE.L) GOTO 30
         WRITE(6,20)J
   30 CONTINUE
      DO 100 I=1,M
         II=FLOAT(I)-1.0
         S=(II-MM/2.0)*D3
         Q=S/H0
         G=1.0 /(1.0 +Q*Q)**2.5
         G=(A2*Q*Q+A1*Q+A0)*G
         IF(J.NE.L) GOTO 90
         GG(I)=G*K1
         IF(I.NE.M) GOTO 80
            M2=M*2
            M3=IFIX(MM*0.5)
            CALL LNORM(1234567,TN,M2,1,0)
            DO 50 K=1,M2
               TN(K)=TN(K)*N
   50       CONTINUE
            DO 60 K=1,M
               TN(K+M3)=TN(K+M3)+GG(K)
   60       CONTINUE
   80    CONTINUE
   90    CONTINUE
         S0=S0+G*G
  100 CONTINUE
      RETURN
      END
C
C  THIS SUBROUTINE RETURNS THE PROB OF DETECTION FOR THE TWO SIGNAL
C  DETECTION THEORY MODELS.
C
      SUBROUTINE PROB1(S0,K,V6,K1,S1,M,V7,D1,D2,E)
C
      INTEGER M,E
      REAL    S0,V6,K(1000),K1,V7,D1(1000),D2(1000),Y,S1
      REAL    K2,V8,MM,A3,L0,B3,V9
C
      K2=SQRT(S0)
      K(E)=K2
      V8=-V6+K1*K2/S1
      L0=K1*K1*SC/(S1*S1)
      MM=FLOAT(M)
      A3=MM+L0
```

```
      B3=1.0 +LO/(MM+LO)
      V9=-SQRT(2.C *V7/B3)+SQRT(2.0 *A3/B3-1.0 )
C
      CALL IFROB(V8,Y)
         D1(E)=Y
      CALL IFROB(V9,Y)
         D2(E)=Y
      RETURN
      END
C
C   THIS SUBROUTINE RETURNS THE ANGLE AND MAGNITUDE OF A VECTOR SUM.
C
      SUBROUTINE ROTATE (U,V,J,K)
      REAL   K,U,V,J
C
      K=SQRT(U*U+V*V)
      IF(K.EQ.0.C ) GOTO 1C
         J=ATAN2(U,V)
         GOTC 20
 10   CONTINUE
      J=0.0
 2C   CONTINUE
      RETURN
      END
C
C   THIS SUBROUTINE RETURNS Z GIVEN F(Z) FOR THE NORMAL PROBABILITY FCN.
C
      SUBROUTINE INORM1(X,Y)
C
      REAL   Y,GC,G1,G2,H1,H2,H3,X
C
      Y=X
      IF(X.GT.0.5 ) Y=1.0 -Y
      Y=SQRT(LOG(1.0 /Y/Y))
      GC=2.515517
      G1=0.8C2853
      G2=0.010328
      H1=1.432788
      H2=0.189269
      H3=0.001308
      Y=Y-(GC+Y*(G1+Y*G2))/(1.0 +Y*(H1+Y*(H2+H3*Y)))
      IF(X.GT.0.5 ) Y=-Y
      RETURN
      END
C
C   THIS SUBROUTINE RETURNS F(Z) GIVEN Z FOR THE NORMAL PROB FCN.
C
      SUBROUTINE IPROB(X,Y)
```

```
C
      REAL    X,Y,W,Q1,Q2,Q3,Q4,Q5,PI,YY
C
      Y=X
      IF(X.LT.0.C ) Y=-Y
      W=1.0 /(1.0 +0.2316419 *Y)
      Q1=0.31938153
      Q2=-0.356563782
      Q3=1.781477937
      Q4=-1.821255978
      Q5=1.330274429
      IF(Y.GT.15.C) GOTC 100
         PI=3.141592654
         YY=W*(Q1+W*(Q2+W*(Q3+W*(Q4+W*Q5))))/SQRT(2.0*PI)
         Y=EXP(-(Y*Y/2.0))*YY
         GOTC 11C
  100 CCNTINUE
      Y=0.0
  110 CCNTINUE
      IF(X.GE.0.C ) Y=1.0 -Y
      RETURN
      END
C
C   THIS SUBROUTINE RETURNS THE PROBABILITY OF DET FCR THE OPTEVFOR MODEL
C
      SUBROUTINE MCD3(M,N,CRF,AL,L9,D5,E,V)
C
      INTEGER E
      REAL M,N,CFF,AL,L9,D5(500),RH,C,SIG,Z,Y,P,V
C
      C=0.10
      P=1.0/3.0
      RH=(C*M/(CFF*N))**P
      SIG=AL*RH
      P=(L9**2 + V**2)**0.5
      Z=(RH-P)/SIG
      CALL IPROB(Z,Y)
      D5(E)=Y
      RETURN
      END
```

LTR ANG	PD(CC)	PD(SL)	PD(OP)	G(I)	TN(I)
-1500.0	0.054	0.016	0.0	0.0114	0.1110
-1470.0	0.058	0.016	0.000	0.0140	-0.0488
-1440.0	0.063	0.016	0.000	0.0173	-0.1709
-1410.0	0.068	0.017	0.000	0.0212	0.0289
-1380.0	0.074	0.017	0.000	0.0259	-0.0325
-1350.0	0.081	0.017	0.000	0.0316	-0.0464
-1320.0	0.089	0.018	0.000	0.0383	-0.0529
-1290.0	0.098	0.018	0.000	0.0462	-0.0660
-1260.0	0.110	0.019	0.000	0.0553	-0.0693
-1230.0	0.123	0.020	0.000	0.0655	0.0036
-1200.0	0.139	0.021	0.000	0.0766	0.0074
-1170.0	0.159	0.022	0.000	0.0882	0.0248
-1140.0	0.182	0.024	0.000	0.0996	0.0406
-1110.0	0.210	0.026	0.000	0.1100	-0.0868
-1080.0	0.245	0.029	0.000	0.1181	-0.0888
-1050.0	0.287	0.032	0.000	0.1229	-0.1846
-1020.0	0.337	0.036	0.000	0.1232	-0.0197
-990.0	0.398	0.043	0.000	0.1185	-0.0663
-960.0	0.469	0.051	0.000	0.1089	0.0341
-930.0	0.550	0.063	0.000	0.0951	0.0156
-900.0	0.640	0.080	0.000	0.0784	0.0616
-870.0	0.733	0.105	0.000	0.0604	0.0129
-840.0	0.823	0.143	0.000	0.0427	0.0901
-810.0	0.898	0.199	0.000	0.0265	0.0352
-780.0	0.953	0.282	0.000	0.0127	0.1639
-750.0	0.984	0.401	0.000	0.0016	0.0253
-720.0	0.996	0.557	0.000	-0.0069	0.0169
-690.0	1.000	0.733	0.000	-0.0130	0.0202
-660.0	1.000	0.886	0.000	-0.0170	-0.1250
-630.0	1.000	0.972	0.000	-0.0195	-0.1027
-600.0	1.000	0.997	0.000	-0.0207	-0.0647
-570.0	1.000	1.000	0.001	-0.0210	0.1751
-540.0	1.000	1.000	0.004	-0.0207	0.2397
-510.0	1.000	1.000	0.011	-0.0199	0.1687
-480.0	1.000	1.000	0.027	-0.0189	0.1137
-450.0	1.000	1.000	0.059	-0.0178	0.1273
-420.0	1.000	1.000	0.116	-0.0166	0.1432
-390.0	1.000	1.000	0.201	0.0	0.1815
-360.0	1.000	1.000	0.314	0.0	-0.1059
-330.0	1.000	1.000	0.444	0.0	0.0659
-300.0	1.000	1.000	0.578	0.0	0.1731
-270.0	1.000	1.000	0.700	0.0	0.0912
-240.0	1.000	1.000	0.799	0.0	0.1020
-210.0	1.000	1.000	0.872	0.0	-0.0259
-180.0	1.000	1.000	0.922	0.0	-0.1378
-150.0	1.000	1.000	0.953	0.0	-0.0262
-120.0	1.000	1.000	0.971	0.0	0.0956
-90.0	1.000	1.000	0.981	0.0	0.1121
-60.0	1.000	1.000	0.987	0.0	-0.0009
-30.0	1.000	1.000	0.989	0.0	-0.0580
0.0	1.000	1.000	0.990	0.0	0.0091
30.0	1.000	1.000	0.989	0.0	-0.0750
60.0	1.000	1.000	0.987	0.0	-0.0543
90.0	1.000	1.000	0.981	0.0	0.0105
120.0	1.000	1.000	0.971	0.0	-0.0000
150.0	1.000	1.000	0.953	0.0	0.0766
180.0	1.000	1.000	0.922	0.0	-0.0412
210.0	1.000	1.000	0.872	0.0	0.0262
240.0	1.000	1.000	0.799	0.0	0.0057
270.0	1.000	1.000	0.700	0.0	-0.0360
300.0	1.000	1.000	0.578	0.0	-0.1266
330.0	1.000	1.000	0.444	0.0	0.1146
360.0	1.000	1.000	0.314	0.0	-0.1353
390.0	1.000	1.000	0.201	0.0	-0.0248
420.0	1.000	1.000	0.116	0.0	-0.1144
450.0	1.000	1.000	0.059	0.0	-0.0815

480.0	1.000	1.000	0.027	0.0	0.1360
510.0	1.000	1.000	0.011	0.0	0.0004
540.0	1.000	0.990	0.004	0.0	0.2016
570.0	1.000	0.925	0.001	0.0	0.0730
600.0	1.000	0.765	0.000	0.0	-0.1205
630.0	0.996	0.561	0.000	0.0	0.1280
660.0	0.980	0.381	0.000	0.0	-0.0528
690.0	0.938	0.251	0.000	0.0	-0.0106
720.0	0.862	0.167	0.000	0.0	0.0
750.0	0.761	0.115	0.000	0.0	0.0
780.0	0.650	0.082	0.000	0.0	0.0
810.0	0.543	0.062	0.000	0.0	0.0
840.0	0.447	0.048	0.000	0.0	0.0
870.0	0.367	0.039	0.000	0.0	0.0
900.0	0.301	0.033	0.000	0.0	0.0
930.0	0.249	0.029	0.000	0.0	0.0
960.0	0.207	0.026	0.000	0.0	0.0
990.0	0.174	0.023	0.000	0.0	0.0
1020.0	0.148	0.021	0.000	0.0	0.0
1050.0	0.127	0.020	0.000	0.0	0.0
1080.0	0.110	0.019	0.000	0.0	0.0
1110.0	0.096	0.018	0.000	0.0	0.0
1140.0	0.085	0.018	0.000	0.0	0.0
1170.0	0.076	0.017	0.000	0.0	0.0
1200.0	0.068	0.017	0.000	0.0	0.0
1230.0	0.062	0.016	0.000	0.0	0.0
1260.0	0.057	0.016	0.000	0.0	0.0
1290.0	0.052	0.016	0.000	0.0	0.0
1320.0	0.048	0.015	0.000	0.0	0.0
1350.0	0.045	0.015	0.000	0.0	0.0
1380.0	0.042	0.015	0.000	0.0	0.0
1410.0	0.040	0.015	0.000	0.0	0.0
1440.0	0.038	0.015	0.000	0.0	0.0
1470.0	0.036	0.015	0.000	0.0	0.0
1500.0	0.034	0.015	0.0	0.0	0.0

```
10 DIM G(200),D1(100),D2(100),K(100),X0(100)
15 DIM D5(100)
20 DEG
30 PRINT "MAX FREQ";
40 INPUT F1
50 PRINT :PRINT "MAX FREQ = ";F1
60 T1=1/F1
70 PRINT "INTERVAL TIME = ";:INPUT T7
80 G=T7/2/T1
90 H=INT(G)
100 H=H+INT(2*(G-H))
110 M=2*H+1
120 IF M>200 THEN 70
130 PRINT "INT TIME = ";T7
140 T7=T1*M
150 PRINT "ADJ INT TIME = ";T7
160 PRINT "SAMPLE SIZE = ";M
170 PRINT :PRINT "F/A RATE ";
180 INPUT F2
190 PRINT :PRINT "F/A RATE = ";F2
200 P1=F2*(M-1)*T1/3600
210 PRINT "PF = ";P1
220 PRINT :PRINT "INPUT DIP ANGLE (1=YES,0=NO)";:INPUT A
230 IF A=0 THEN 260
240 PRINT "DIP ANGLE PHI ";:INPUT F
250 GOTO 420
260 DEG :L1=76:L2=100
270 PRINT :PRINT "LATITUDE ";
280 INPUT L
290 PRINT :PRINT "LONGITUDE ";
300 INPUT O
310 PRINT :PRINT "LAT = ";L:PRINT "LON = ";O
320 F=SIN(O-L2)*COS(L):G=COS(O-L2)*COS(L):H=SIN(L)
330 U=G:V=H
340 GOSUB 1900
350 J=J-(90-L1):G=K*SIN(J):H=K*COS(J)
360 U=G:V=F
370 GOSUB 1900
380 F=K:G=0:R=-(COS(L1)*SIN(J)):Q=-(COS(L1)*COS(J))
390 U=H:V=F
400 GOSUB 1900
410 F=ATN(2*(SIN(J)/COS(J)))
420 PRINT "PHI = ";F
430 PRINT :PRINT "DIPOLE COURSE ";:INPUT C1:PRINT "DIPOLE SPEED ";:INPUT V1
440 PRINT :PRINT "SENSOR COURSE ";:INPUT C2:PRINT "SENSOR SPEED ";:INPUT V2
450 PRINT "DIPOLE COURSE = ";C1:PRINT "DIPOLE SPEED = ";V1
460 PRINT "SENSOR COURSE = ";C2:PRINT "SENSOR SPEED = ";V2
470 W1=V2*SIN(C2)-V1*SIN(C1):W2=V2*COS(C2)-V1*COS(C1)
480 U=W1:V=W2
490 GOSUB 1900
500 C0=J:W0=K
510 D3=W0*T1*4.63/9
520 PRINT "REL COURSE = ";C0:PRINT "REL SPEED = ";W0
530 PRINT :PRINT "INPUT DIPOLE MOMENT (1=YES,0=NO)";:INPUT AA
540 IF AA=0 THEN 580
550 PRINT :PRINT "MAGNITUDE P ";:INPUT P:PRINT "HOR ANGLE w ";:INPUT A
560 PRINT :PRINT "VERT ANGLE OMEGA ";:INPUT B
570 GOTO 640
580 PRINT :PRINT "INPUT EARTH FIELD (1=YES,0=NO) ";:INPUT AA
```

```
590 IF AA=0 THEN 620
600 PRINT :PRINT "EARTH FIELD ";:INPUT E1
610 GOTO 630
620 E1=70000/SQR(3*COS(F)*COS(F)+1)
630 PRINT :PRINT "EARTH FIELD = ";E1
640 M4=0:M5=0:M6=0
650 PRINT :PRINT "INPUT PERM MOMENTS (1=YES,0=NO) ";:INPUT AA
660 IF AA=0 THEN 690
670 PRINT :PRINT "LONG MOMENT ";:INPUT M4:PRINT "TRAN MOMENT ";:INPUT M5
680 PRINT "VERT MOMENT ";:INPUT M6
690 PRINT :PRINT "LONG MOMENT = ";M4:PRINT "TRAN MOMENT = ";M5:PRINT "VERT MOMEN
T = ";M6
700 K1=7.3:K2=1.6:K3=1.6
710 PRINT :PRINT "DISPLACEMENT ";
720 INPUT N1
730 PRINT :PRINT "DISPLACEMENT = ";N1
735 NN1=N1
740 M9=E1*K3*N1*SIN(F):M3=M9+M6
750 M8=E1*COS(F)*N1*(K1*COS(C1)*COS(C1)+K2*SIN(C1)*SIN(C1))
760 M1=M4*SIN(C1)+M5*COS(C1):M2=M4*COS(C1)-M5*SIN(C1)
770 M7=E1*(COS(F)*(K1-K2)*N1*SIN(C1)*COS(C1))
780 M1=M7+M1:M2=M8+M2
790 U=M1:V=M2
800 GOSUB 1900
810 A=J:U=M3:V=K
820 GOSUB 1900
830 P=K:B=J
840 PRINT :PRINT "P = ";P:PRINT "w = ";A:PRINT "OMEGA = ";B
850 X=P1
860 GOSUB 1920
870 V6=Y
880 V7=M*(1-2/9/M+Y*SQR(2/9/M))^3
890 PRINT :PRINT "VERT SEPARATION ";:INPUT Z
900 PRINT :PRINT "VERT SEPARATION = ";Z
910 PRINT :PRINT "NOISE ";
920 INPUT S1
925 S2=S1*4
930 PRINT :PRINT "NOISE = ";S1
940 PRINT :PRINT "MAX LATERAL RANGE ";:INPUT R8
950 PRINT :PRINT "NUMBER OF INCREMENTS ";:INPUT N7
960 PRINT :PRINT "MAX LATERAL RANGE = ";R8:PRINT "NUMBER OF INCREMENTS = ";N7
964 PRINT :PRINT " ORF ";:INPUT ORF
965 PRINT :PRINT " ORF = ";ORF
970 D4=R8/N7:N8=2*N7
974 PRINT :PRINT " ALPHA ";:INPUT AL
975 PRINT :PRINT " ALPHA = ";AL
980 L9=-R8
990 FOR E=0 TO N8
1000 X0=L9:X0(E)=L9
1010 GOSUB 1620
1020 L9=L9+D4
1030 GOSUB 1800
1040 NEXT E
1044 GOTO 1290
1050 GRAPHICS 8:COLOR 1
1060 XX=INT(310/N8)
1065 X0(0)=0
1070 FOR I=0 TO N8
1080 D1(I)=INT((1-D1(I))*160)
1090 D2(I)=INT((1-D2(I))*160)
1095 D5(I)=INT((1-D5(I))*160)
1100 X0(I+1)=X0(I)+XX
1110 NEXT I
1120 PLOT X0(0),D1(0)
1130 FOR I=1 TO N8
1140 DRAWTO X0(I),D1(I)
```

```
1150 NEXT I
1160 PLOT X0(0),D2(0)
1170 FOR I=1 TO N8
1180 DRAWTO X0(I),D2(I)
1190 NEXT I
1192 PLOT X0(0),D5(0)
1194 FOR I=1 TO N8
1196 DRAWTO X0(I),D5(I)
1198 NEXT I
1200 PRINT "PD FOR X FROM ";-R8;" TO ";R8
1220 GOTO 1610
1230 PRINT "FOR HARD COPY ENTER '1'";:INPUT CC
1295 IF CC()1 THEN GOTO 1050
1300 LPRINT "MAX FREQ = ";F1
1310 LPRINT "ADJ INT TIME = ";T7
1320 LPRINT "SAMPLE SIZE = ";M
1330 LPRINT "F/A RATE = ";F2
1335 LPRINT "PF = ";P1
1340 LPRINT "LAT = ";L
1350 LPRINT "LON = ";O
1360 LPRINT "PHI = ";F
1370 LPRINT "DIPOLE COURSE = ";C1
1380 LPRINT "DIPOLE SPEED = ";V1
1390 LPRINT "SENSOR COURSE = ";C2
1400 LPRINT "SENSOR SPEED = ";V2
1410 LPRINT "REL COURSE = ";C0
1420 LPRINT "REL SPEED =";W0
1430 LPRINT "EARTH FIELD = ";E1
1440 LPRINT "LONG MOMENT = ";M4
1450 LPRINT "TRAN MOMENT = ";M5
1460 LPRINT "VERT MOMENT = ";M6
1470 LPRINT "DISPLACEMENT = ";NN1
1480 LPRINT "P = ";P
1490 LPRINT "w = ";A
1500 LPRINT "OMEGA = ";B
1505 LPRINT "VERT SEPARATION = ";Z
1510 LPRINT "NOISE = ";S1
1515 LPRINT "MAX LATERAL RANGE = ";R8
1520 LPRINT "NUMBER OF INCREMENTS = ";N7
1525 LPRINT :LPRINT "LTR RNG   PD(CC)      PD(SL)      PD(OPT)"
1530 L9=-R8
1535 FOR I=0 TO N8
1540 LPRINT L9;"     ";D1(I);"      ";D2(I);"      ";D5(I)
1545 L9=L9+D4
1550 NEXT I
1560 GOTO 1050
1605 PRINT "END"
1610 END
1620 U=X0:V=Z
1630 GOSUB 1900
1640 D=J:H0=K
1642 RH=(0.1*P/(ORF*S2))^0.333
1643 SIG=AL*RH
1645 X=(RH-H0)/SIG
1646 GOSUB 1990
1647 D5(E)=Y
1650 B0=COS(B)*COS(C0-A):J0=COS(D)*COS(B)*SIN(C0-A)-SIN(D)*SIN(B)
1660 N0=-(SIN(D)*COS(B)*SIN(C0-A))-COS(D)*SIN(B)
1670 B1=COS(F)*COS(C0):J1=COS(D)*COS(F)*SIN(C0)-SIN(D)*SIN(F)
1680 N1=-(SIN(D)*COS(F)*SIN(C0))-COS(D)*SIN(F)
1690 K1=P/10/H0^3
1700 A2=2*B0*B1-J0*J1-N0*N1:A1=3*(N0*B1+B0*N1):A0=2*N0*N1-B0*B1-J0*J1
1710 S0=0
1720 FOR I=0 TO M-1
1730 S=(I-(M-1)/2)*D3
1740 Q=S/H0
```

```
1750 G=1/(1+Q*Q)^2.5
1760 G=(A2*Q*Q+A1*Q+A0)*G
1770 G(I)=G:S0=S0+G*G
1780 NEXT I
1790 RETURN
1800 K2=SQR(S0)
1810 K(E)=K2
1820 V8=-V6+K1*SQR(S0)/S1
1830 L0=K1*K1*S0/(S1*S1):A3=M+L0:B3=1+L0/(M+L0)
1840 V9=-SQR(2*V7/B3)+SQR(2*A3/B3-1)
1850 X=V8:GOSUB 1990
1860 D1(E)=Y
1870 X=V9:GOSUB 1990
1880 D2(E)=Y
1890 RETURN
1900 K=SQR(U*U+V*V):IF K=0 THEN J=0:RETURN
1905 UK=U/K:VK=V/K
1907 IF UK)0.999999 AND VK)0.999999 THEN J=0:RETURN
1908 IF UK)0.999999 THEN J=-ATN(VK/SQR(-VK*VK+1))+90:RETURN
1909 IF VK)0.999999 THEN J=0:RETURN
1910 MM=ATN(UK/SQR(-UK*UK+1)):J=-ATN(VK/SQR(-VK*VK+1))+90:IF MM(0 THEN J=360-J
1915 RETURN
1920 Y=X:IF X)0.5 THEN Y=1-Y
1930 Y=SQR(LOG(1/Y/Y))
1940 G0=2.515517:G1=0.802853:G2=0.010328
1950 H1=1.432788:H2=0.189269:H3=1.308E-03
1960 Y=Y-(G0+Y*(G1+G2*Y))/(1+Y*(H1+Y*(H2+H3*Y)))
1970 IF X)0.5 THEN Y=-Y
1980 RETURN
1990 Y=X:IF X(0 THEN Y=-Y
2000 W=1/(1+0.2316419*Y)
2010 Q1=0.31938153:Q2=-0.356563782:Q3=1.78147793:Q4=-1.82122559:Q5=1.33027442
2020 IF Y)24.23 THEN Y=0:GOTO 2070
2025 PI=3.14159265
2030 Y=EXP(-(Y*Y/2))/SQR(2*PI)*W*(Q1+W*(Q2+W*(Q3+W*(Q4+W*Q5))))
2070 IF X)0 THEN Y=1-Y
2075 Y=(INT(10000*Y))/10000
2080 RETURN
```

```
MAX FREQ = 1.8
ADJ INT TIME = 20.55555555
SAMPLE SIZE = 37
F/A RATE = 3
PF = 0.0166666666
LAT = 30
LON = 60
PHI = 59.40076979
DIPOLE COURSE = 45
DIPOLE SPEED = 10
SENSOR COURSE = 315
SENSOR SPEED = 220
REL COURSE = 312.397439
REL SPEED =220.227153
EARTH FIELD = 52506.5513
LONG MOMENT = 0
TRAN MOMENT = 0
VERT MOMENT = 0
DISPLACEMENT = 4000
P = 6734694892
w = 32.63750751
OMEGA = 27.11173179
VERT SEPARATION = 200
NOISE = 0.1
MAX LATERAL RANGE = 1500
NUMBER OF INCREMENTS = 15

LTR RNG    PD(CC)      PD(SL)      PD(OPT)
-1500     0.0544      0.0158      0
-1400     0.0696      0.0166      0
-1300     0.0948      0.0181      0
-1200     0.1391      0.0209      0
-1100     0.2212      0.0266      0
-1000     0.3765      0.0403      0
-900     0.6399      0.0801      0
-800     0.9191      0.2233      0
-700     0.999      0.6743      0
-600     1      0.9973      2E-04
-500     1      1      0.0133
-400     1      1      0.1605
-300     1      1      0.567
-200     1      1      0.8868
-100     1      1      0.9774
0     1      1      0.9898
100     1      1      0.9774
200     1      1      0.8868
300     1      1      0.567
400     1      1      0.1605
500     1      0.9999      0.0133
600     0.9997      0.7654      2E-04
700     0.9157      0.2189      0
800     0.5775      0.0677      0
900     0.3014      0.0331      0
1000     0.1644      0.0226      0
1100     0.1003      0.0184      0
1200     0.0683      0.0165      0
1300     0.0508      0.0156      0
1400     0.0405      0.0151      0
1500     0.034      0.0148      0
```

LIST OF REFERENCES

1. Urick, R.J., Principles of Underwater Sound, 2d ed., McGraw-Hill, 1975.

2. Naval Postgraduate School Report NPS55-77-19, Magnetic Anomaly Detection Models, by R.N. Forrest, April 1977.

3. Naval Postgraduate School Report NPS55-83-032, MAD Detection and the Naval Warfare Gaming System, by R.N. Forrest, November 1983.

4. U.S. National Defense Research Committee, Magnetic Airborne Detector Program, v. 5, 1946.

5. Operational Test and Evaluation Force, First Partial Report on Project O/V67, Conduct an Operational Evaluation of the IMS (Integrated MAD System), 21 April 1969.

6. Texas Instruments Incorporated Report C2-61009-2, MAD Signal Processing Study Report No. 2 Analytical Report, v. 1, 1 April 1961.

7. Defense Mapping Agency Hydrographic Center Chart Number 39, Total Intensity of the Earth's Magnetic Field, EPOC 1975.0, 4th ed., December 1975.

8. Defense Mapping Agency Hydrographic Center Chart Number 30, Magnetic Inclination or Dip, EPOC 1975.0, 9th ed., November 1975.

9. Naval Postgraduate School Report NPS55-78-021 (Revised), Magnetic Anomaly Detection Models with a Program for a Texas Instruments TI-59 Calculator, by R.N. Forrest, September 1978, rev. September 1983.

10. Phoenix Corporation Report AFGL-TR-80-0243, An Overview of Geomagnetic Field Models, by R.D. Regan, 15 August 1980.

11. Barger, M.I. and Schemmer, B.F., "ASW Goes Inboard for Swifter, Surer Hunt," Armed Forces Journal International, February 1984.

12. Naval Postgraduate School Report NPS55-81-005, The New Naval Postgraduate School Random Number Package--LLRANDOMII, by P.A.W. Lewis, February 1981.

13. Anti-Submarine Warfare Systems Project Office Memorandum 71-12, APAIR MOD 2.6, v. 1, July 1971.

14. Combat Fleets of the World 1982/1983, 4th ed., Naval Institute Press, 1982.

INITIAL DISTRIBUTION LIST

		No. Copies
1.	Defense Technical Information Center Cameron Station Alexandria, Virginia 22314	2
2.	Library, Code 0142 Naval Postgraduate School Monterey, California 93943	2
3.	Commander Submarine Development Squadron 12 Naval Submarine Base, New London Groton, Connecticut 06340	1
4.	Commanding Officer Attn: Code 713 Air Test and Evaluation Squadron 1 (VX-1) Patuxent River, Maryland 20670	1
5.	Commander Code 3012 Naval Air Development Center Warminster, Pennsylvania 18974	1
6.	Commander Library Naval Air Development Center Warminster, Pennsylvania 18974	1
7.	R.N. Forrest, Code 55Fo Department of Operations Research Naval Postgraduate School Monterey, California 93943	3
8.	A.F. Andrus, Code 55As Department of Operations Research Naval Postgraduate School Monterey, California 93943	1
9.	M.G. Sovereign, Code 74 Department of Command, Control and Communications Naval Postgraduate School Monterey, California 93943	1

10. Director 1
Code 331AA
Center for Wargaming
Newport, Rhode Island 02840

11. Commander 1
Naval Electronic Systems Command
Attn: PME 120
2511 Jefferson Davis Highway
Arlington, Virginia 20360

12. Commander, Code 370 1
Naval Air Systems Command
1411 Jefferson Davis Highway
Arlington, Virginia 20361

13. White Oak Laboratory 1
Naval Surface Weapons Center
Silver Spring, Maryland 20910

14. Newport Laboratory 1
Naval Underwater Systems Center
Newport, Rhode Island 02840

15. New London Laboratory 1
Naval Underwater Systems Center
New London, Connecticut 06320

16. Commander 1
Naval Ocean Systems Center
San Diego, California 92152

17. Commanding Officer, Code NISC 20 1
4301 Suitland Road
Washington, D.C. 20390

18. Commanding Officer 1
Navy Research Laboratory
Washington, D.C. 20375

19. Center for Naval Analysis 1
2000 N. Beauregard St.
Arlington, Virginia 22311

20. Lcdr Dick Grahlman 1
Air Officer
USS Ponce (LPD-15)
FPO, New York 09582

21. Lt Daniel C. Schluckebier 2
Asst. CATC
USS Dwight D. Eisenhower (CVN-69)
FPO, New York 09532

22. Commander 1
David W. Taylor
Naval Ship Research and Development Center
Bethesda, Maryland 20817

Thesis
S33713 Schluckebier
c.1 A comparison of three
Magnetic Anomally De-
tection (MAD) models.